

Electronic Supplementary Information (ESI) for

Photo-thermal oxidation of single layer graphene

Ahmad E. Islam,^{1,2} Steve S. Kim,^{1,3} Rahul Rao,^{1,3} Yen Ngo,^{1,3} Jie Jiang,¹ Pavel Nikolaev,^{1,3} Rajesh Naik,⁴ Ruth Pachter,¹ John Boeckl,¹ and Benji Maruyama¹

¹Materials and Manufacturing Directorate, Air Force Research Laboratory,

Wright-Patterson Air Force Base, Dayton, OH 45433

²National Research Council, Washington DC 20001

³Biological and Nanoscale Technologies, UES, Inc., Dayton, OH 45432

⁴711th Human Performance Wing, Air Force Research Laboratory,

Wright-Patterson Air Force Base, Dayton, OH 45433

Section S1: Sample Preparation

Silicon Pillar Formation and Oxidation: A series of 10 μm tall and 10 μm diameter silicon (Si) pillars were formed on a silicon-on-insulator (SOI) substrate (having a top-Si layer thickness of $\sim 10 \mu\text{m}$ and a buried oxide thickness of $\sim 1 \mu\text{m}$) in photo-lithographically defined areas. To obtain these Si micro-pillars, SOI substrates with photo-lithographic patterns were subjected to deep reactive ion etching, which is known as the Bosch process with cyclic application of sulphur hexafluoride SF_6 and octafluorocyclobutane C_4F_8 . The pillars are arranged in patches on the substrate; each patch contains an array of 5x5 pillars with $\sim 50 \mu\text{m}$ spacing between them. The pillars (along with the rest of the substrate) contained $\sim 3 \text{ nm}$ native oxide (measured using Ellipsometry). The oxide thickness was increased up to $\sim 90 \text{ nm}$ by oxidizing the substrate in ambient air at 900°C for $\sim 4 \text{ hrs}$ to ensure constructive interference of Raman signals¹ collected using the 532 nm laser.

Graphene Growth: A tube furnace (OTF-1200x-STM, MTI Corp., CA) equipped with a scroll vacuum pump was used for chemical vapor deposition (CVD) of single-layer graphene (SLG). A $1 \times 1 \text{ inch}^2$ copper (Cu) foil was placed in the furnace and was heated up to 1000°C at a pressure of 125 mTorr maintained with a fixed flow of hydrogen. The hydrogen-only reduction step continued for 30 min at 1000°C , which is followed with a flow of methane at a pressure of 1.25 Torr for 30 min at 1000°C . The furnace was cooled down to room temperature while keeping the flow of methane and hydrogen. After completion of the growth, SLG was observed on both sides of the Cu foil.

Graphene Transfer: Fig. S1 shows the schematic of the SLG transfer process on to silicon micro-pillars. A thermal release (TR) tape (125°C release; Nitto Americas Inc., CA) was carefully

placed with no entrapped air bubbles over one side of the Cu foil coated with SLG. SLG present on the other side of the Cu foil was removed using a 5 min O_2 plasma treatment at 35 mW RF power. The placement of TR tape with the SLG on Cu foil in $Fe(NO_3)_3$ solution (made with 50 mg diluted in 1 ml of deionized DI water) for ~ 4 hrs etched away Cu and left SLG on TR tape, which was later rinsed with DI water and blow-dried with N_2 . The tape with SLG was adhered to the substrate with silicon micro-pillars at room temperature. The tape was later released by heating the substrate at 125°C for 1-2 min. The tape and other organic residues were removed from the substrate using forming gas (10% H_2 ; Ar balance) anneal at 400 °C for ~ 4 hrs. The process leaves SLG on the micro-pillars of the substrate (along with other unanalyzed regions that the tape adhered to) for subsequent chemical modification.

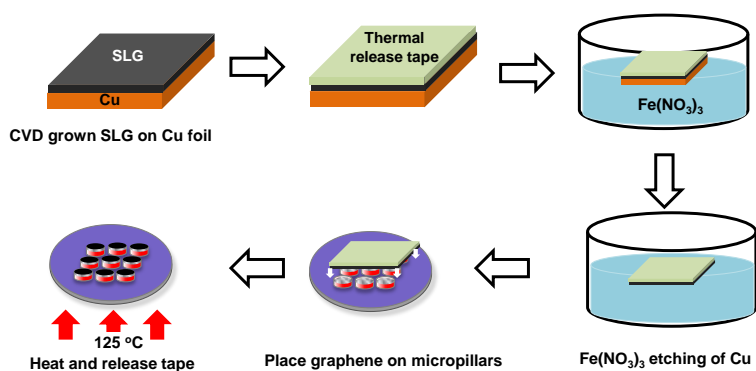
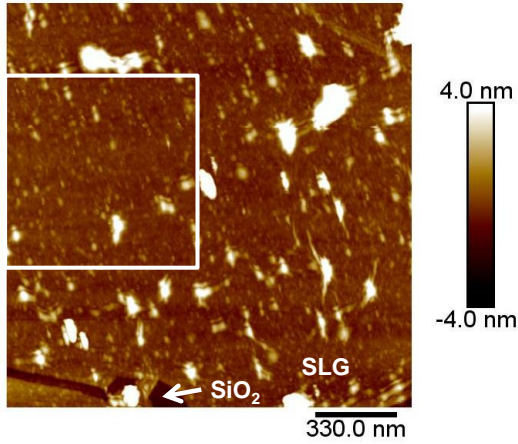


Fig. S1 Schematic representation of the transfer process of single-layer graphene (SLG) from Cu foil to silicon substrates with micro-pillars.

(a) AFM height profile



(b) AFM phase profile

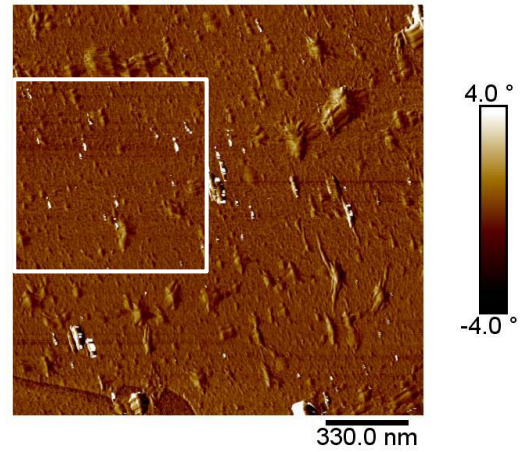


Fig. S2 Surface topography of SLG before oxidation obtained using Atomic Force Microscopy (AFM). AFM (a) height and (b) phase profiles of SLG placed on top of a micro-pillar. Areas imaged in Figs. 2(a) and 3(a) are marked using square boxes in Figs. (a) and (b), respectively. The bright spots in the AFM profiles represent residues from the SLG transfer process. As SLG has incomplete coverage on the micro-pillars, SiO₂ is exposed in some part of the image as marked in Fig. (a).

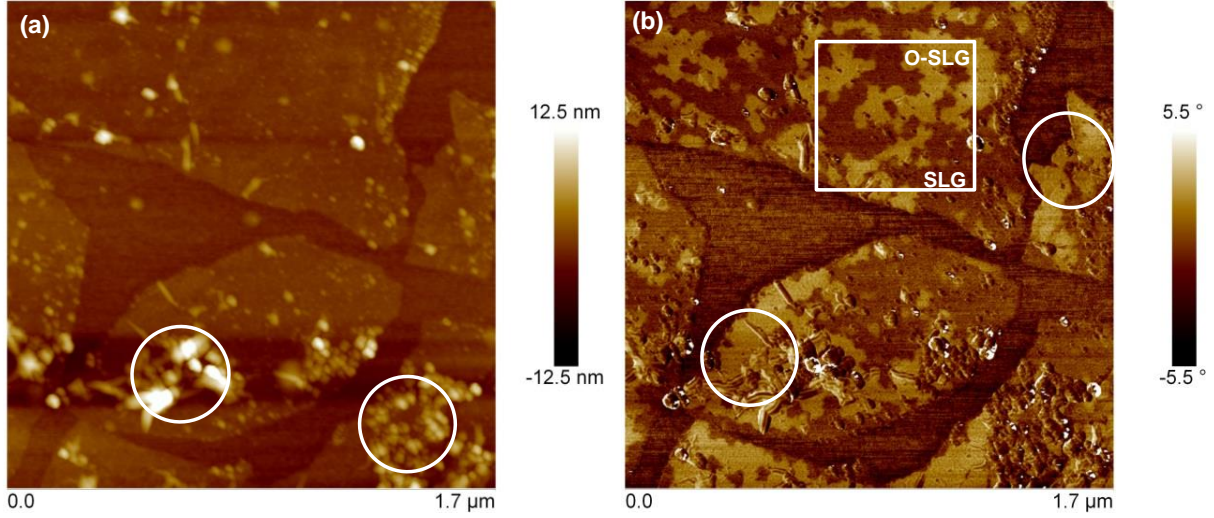


Fig. S3 AFM (a) height and (b) phase profiles on top of a micro-pillar after SLG oxidation at $T \sim 678$ °C using $p(\text{O}_2) \sim 2.5$ Torr for $t \sim 150$ s. Presence of transfer residues (highlighted using circles in Fig. (a)) do not influence SLG oxidation, as similar degrees of oxidation are observed in SLGs with and without residues (highlighted using circles in Fig. (b)). Areas imaged in Fig. 3b is marked using a square box in Fig. (b).

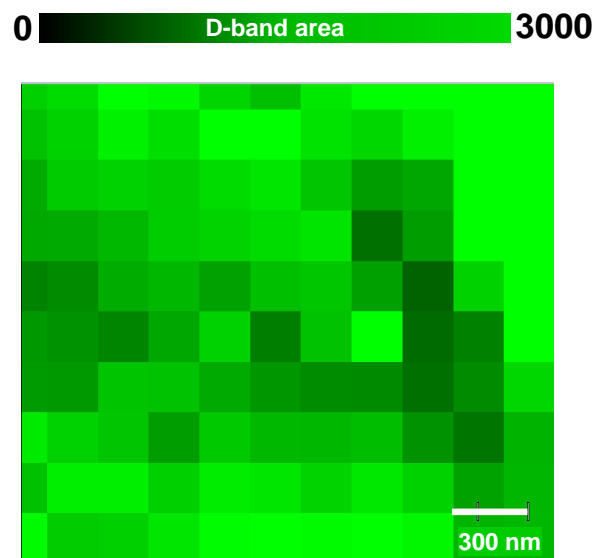


Fig. S4 Two-dimensional map of D-band for the regions profiled in Fig. S3. As the laser spot size is $\sim 1 \mu\text{m}$, the oxidized (O-SLG) and pristine (SLG) domains cannot be distinguished in the Raman profile.

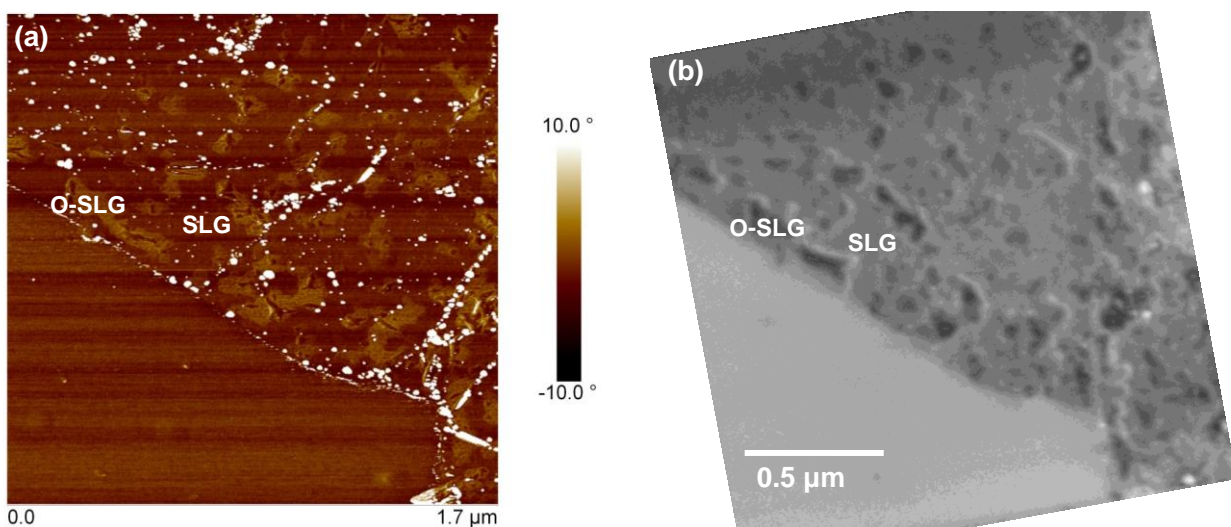


Fig. S5 Comparison of (a) AFM phase profile and (b) SEM image (performed using $\sim 1 \text{ kV}$ acceleration voltage) of oxidized SLG. Oxidation is performed here at $T \sim 653^\circ\text{C}$ and at $p(\text{O}_2) \sim 2.5 \text{ Torr}$. The oxidized areas (O-SLG; with higher phase in the AFM scan) appear darker in the

SEM image compared to the non-oxidized areas, which suggests O-SLG regions have lower conductivity.

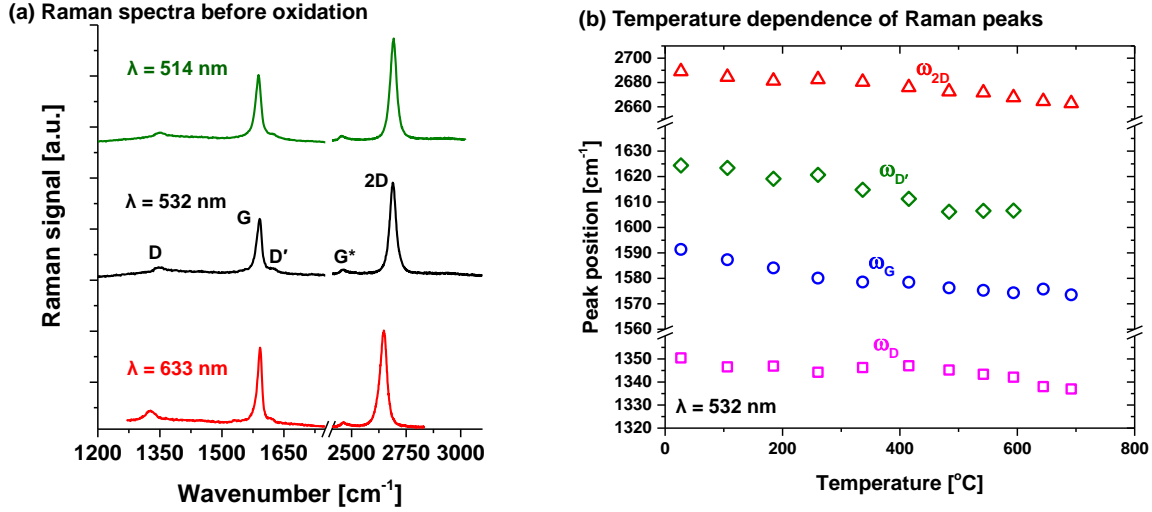


Fig. S6 Raman analysis of SLG before oxidation. (a) Raman spectra collected from SLG at room temperature using different excitation wavelengths ($\lambda = 514, 532, 633$ nm). Representative Raman bands (D, G, D', G*, and 2D-bands) are marked for the 532 nm spectrum. The spectra show G-band peak at $\sim 1588, 1591, 1592$ cm^{-1} , 2D-band peak at $\sim 2691, 2689, 2647$ cm^{-1} and G*-band peak at $\sim 2455, 2460, 2463$ cm^{-1} at $\lambda = 514, 532, 633$ nm, respectively; the 2D/G peak ratios are $\sim 1.6, 1.73$ and 1.29 (after background subtraction) for the wavelengths under study. Additional peaks at $\sim 1353, 1350, 1327$ cm^{-1} (the D-band; with D/G ratio ~ 0.1) and at $\sim 1626, 1624, 1621$ cm^{-1} (the D'-band; with D/D' ratio ~ 2) measured at the three wavelengths are possibly related to defects present at the edges of the SLG patches after the incomplete SLG transfer to micro-pillars. (b) A plot of temperature dependence of the D, G, D', and 2D-band peak frequencies ($\omega_D, \omega_G, \omega_{D'}$ and ω_{2D}) using $\lambda = 532$ nm excitation. To collect these temperature dependent data, samples containing SLG were placed inside TS-1500 Linkam stage

and kept at ~ 20 Torr Ar ambient. The frequencies for all these Raman bands red-shift (i.e. shift towards lower wavenumber) with the increase in temperature. In literature, only one article has reported shifts in G-band peak over such a broad temperature range² (while others report measurements over a small range of temperature^{3,4}), which is consistent with our measurement.

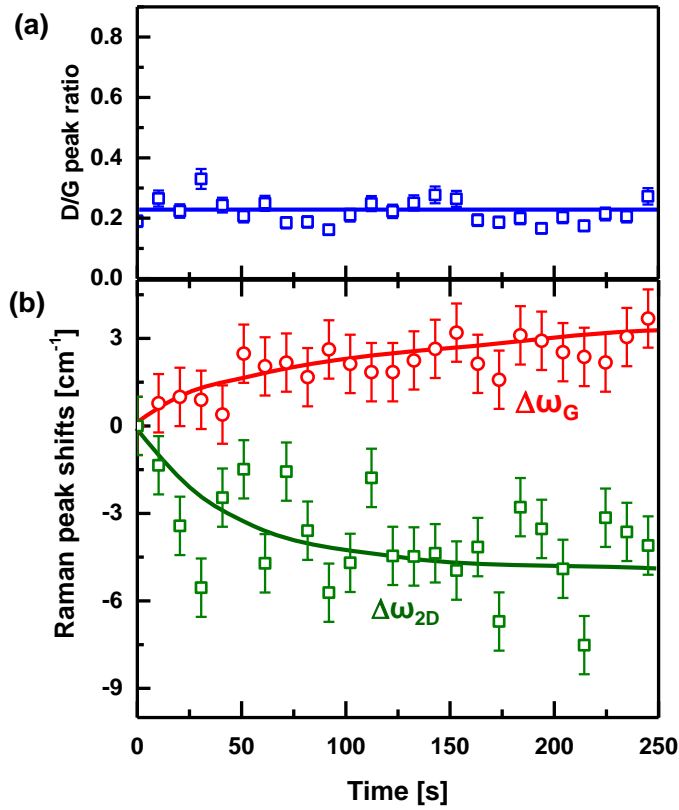


Fig. S7 Results from annealing of SLG at ~ 300 °C under vacuum (0.1 mTorr). In-situ Raman data suggests (a) negligible change in the D/G peak ratio and (b) a monotonous change in the G- and 2D-band peak frequencies (ω_G and ω_{2D}) from its pre-oxidation value. The blue-shift in ω_G and red-shift in ω_{2D} suggests desorption of $-\text{OH}$ groups from SLG and a resultant n-doping.⁵

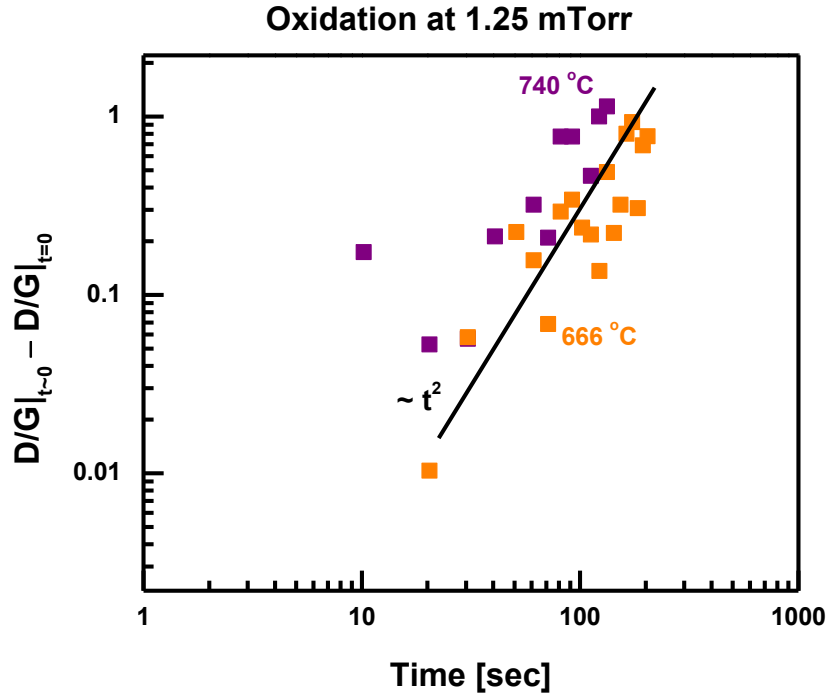


Fig. S8 Time dependence of $(D/G|_{t \sim 0} - D/G|_0)$ during oxidation of SLG measured at $p(\text{O}_2) \sim 1.25$ mTorr and at temperatures 660-740 °C. The solid line suggests $\sim t^2$ dependence for the initial stage of oxidation supporting the $L_D \sim 1/t$ assumption in equation (2) of the main text.

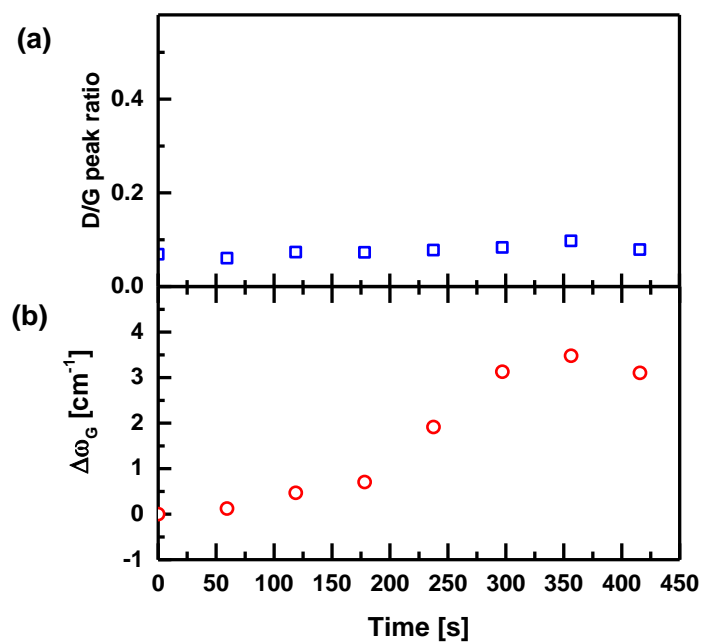


Fig. S9 In-situ Raman data suggests (a) negligible change in the D/G peak ratio and (b) an increase (blue-shift) in the G-band peak from its pre-oxidation value, when SLG is exposed at $\sim 650^\circ\text{C}$ in a Linkam stage with $p(\text{O}_2) \sim 5$ Torr.

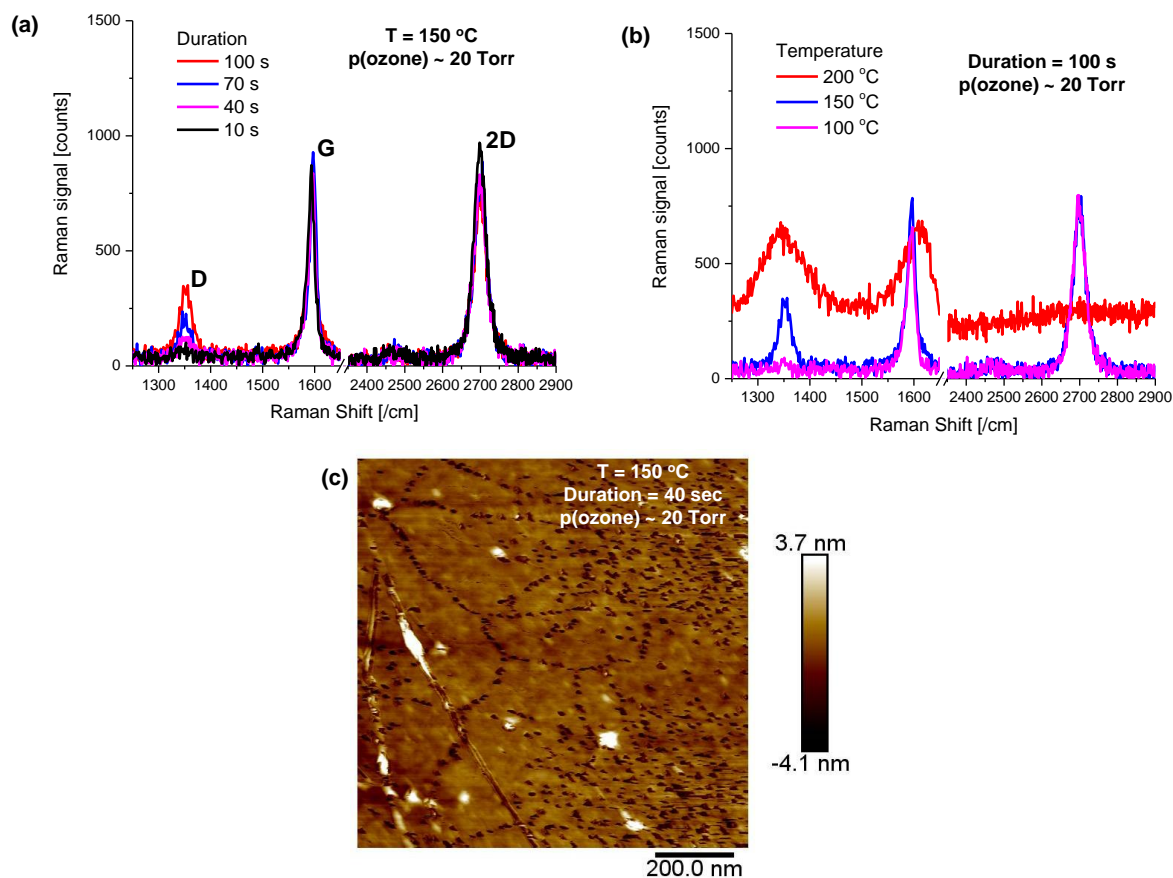


Fig. S10 Results from ozone exposure of SLG at a partial pressure of $\sim 20\text{ Torr}$. Ozone was generated using a DEL ZONE®-LG-7 ozone generator with a flow of 13.5 psi O_2 . Generated ozone was flown into a vacuum chamber containing samples with SLG. The ex-situ Raman data suggests significant increase in D-band Raman signal and an eventual disappearance of 2D-band signal after SLG is exposed to ozone - (a) for different durations at a fixed temperature and (b) for a fixed duration at different temperatures. (c) AFM height profile after ozone treatment of SLG shows significant presence of pores (the black spots).

REFERENCES

1. Y. Y. Wang, Z. H. Ni, Z. X. Shen, H. M. Wang and Y. H. Wu, *Applied Physics Letters*, 2008, **92**.
2. M. R. Joya, A. R. Zanatta and J. Barba-Ortega, *Modern Physics Letters B*, 2013, **27**.
3. I. Calizo, I. Bejenari, M. Rahman, G. Liu and A. A. Balandin, *Journal of Applied Physics*, 2009, **106**.
4. I. Calizo, S. Ghosh, W. Bao, F. Miao, C. N. Lau and A. A. Balandin, *Solid State Communications*, 2009, **149**, 1132-1135.
5. A. Das, S. Pisana, B. Chakraborty, S. Piscanec, S. K. Saha, U. V. Waghmare, K. S. Novoselov, H. R. Krishnamurthy, A. K. Geim, A. C. Ferrari and A. K. Sood, *Nature Nanotechnology*, 2008, **3**, 210-215.